

Solid Fuel Ramjet Simulator Results: Experiment and Analysis in Cold Flow

J. Richardson,* W.A. de Groot,* J.I. Jagoda,† R.E. Walterick,‡ J.E. Hubbart,§ and W.C. Strahle¶
Georgia Institute of Technology, Atlanta, Georgia

This paper presents laser-based experimental results and analytical results on two-dimensional backward-facing step flows with mass injection from the bottom wall behind the step. The facility simulates the flowfield in the flame stabilization region of a solid fueled ramjet. Measured are two components of velocity and shear stress with and without secondary air injection. The same quantities are calculated for foreign-gas injection. The most notable effect of blowing, both experimentally and analytically, is the appearance of a second recirculation zone. Analytically and experimentally, it is found that the general size of the main recirculatory region diminishes with increased blowing rate and that blowoff of the recirculation zone can occur at relatively low blowing rates. This indicates that flame stabilization may be strongly affected by the actual blowing rate in a solid fuel ramjet (SFRJ).

Nomenclature

C_i	= mass fraction of species i
C_μ	= turbulence constant
E	= constant in law of the wall
H	= step height
k	= turbulence kinetic energy
u_i	= velocity in the x_i th coordinate direction
u_τ	= friction velocity
V_0	= injection velocity
x, y	= coordinates
\bar{y}	= wall distance in law of the wall relations
ϵ	= turbulence energy dissipation
κ	= von Kármán constant
μ	= molecular viscosity
μ_T	= turbulent viscosity
ν	= kinematic viscosity
ρ	= density
σ_c	= turbulent (and laminar) Schmidt number (= 0.9)
τ_w	= shear stress

Superscripts and Subscripts

(—)	= conventional time average
+	= nondimensionalized variables in law of the wall
0	= wall value

Introduction

SOLID fueled ramjets operate by ingestion of air and subsequent combustion with a solid fuel.¹ A low-velocity region of flow near the head end of the fuel grain is imperative for flame stabilization. This may be achieved by creating a backward-facing step at the flow boundary, thereby forcing a recirculation zone behind the step. In practice, the flow is

highly turbulent and, even without combustion, is highly complex.

A goal at this laboratory is to compute the solid fueled ramjet flowfield to an accuracy commensurate with establishing scaling laws for quantities such as the flame blowoff limit and fuel regression rate. To this end, a facility has been developed to simulate a solid fueled ramjet flame stabilization region.

In the case of pure two-dimensional cold flow over a backward-facing step, there has been considerable work by a number of investigators, and a recent review article² summarizes this work. Such a flow was labeled as a standard flow with a number 0420 assigned to it in Ref. 3. Reference 4 added to the data base, using intrusive probes where possible. However, this flow is not particularly amenable to intrusive probe testing because there are reversed flow regions and the turbulence velocities can oscillate between positive and negative values. As a consequence, a laser velocimetry (LV) system has been used here.

For the solid fueled ramjet, a unique aspect of the flowfield is that there is mass addition from the wall. Questions that this introduces include issues of movement of the reattachment point, creation of multiple recirculation zones, destabilization of the flowfield, and change in mixing rates. There is also the issue of calculability of the flow when the wall-blowing case is considered. In this paper an LV system is used together with a k - ϵ calculation method to investigate the effects of blowing at the wall with injection velocities typical of those in a solid fueled ramjet. At the present time, cold flow is considered and the sole injectant has been air. However, the calculations also consider foreign-gas injection.

Facility

The tunnel has been described elsewhere,⁴ but it is a suction-type tunnel, drawing air from the quiescent laboratory air. It is shown in Fig. 1. Optical access is provided by optical-glass side walls. Because this tunnel draws air from an irrotational quiescent flow, and because the inlet run to the step is not long enough for the top and bottom wall boundary layers to merge, there should be a potential core to the flow at the step station. It was noted in Ref. 4, however, and confirmed in this work, that there is a freestream "turbulence" level of 2%. This cannot be turbulence but must be an unsteady potential flow. That is, it is acoustics generated by a noisy downstream flow.

Flows over backward-facing steps are notoriously unsteady and are strongly facility-dependent.⁵ Therefore, it is believed necessary here to present the acoustical spectrum obtained by

Presented as Paper 85-0329 at the AIAA 23rd Aerospace Sciences Meeting, Reno, NV, Jan. 14-17, 1985; received Jan. 22, 1985; revision received July 10, 1985. Copyright © American Institute of Aeronautics and Astronautics, Inc., 1985. All rights reserved.

*Graduate Research Assistant, School of Aerospace Engineering.

†Associate Professor, School of Aerospace Engineering. Member AIAA.

‡Research Engineer, School of Aerospace Engineering. Member AIAA.

§Professor, School of Aerospace Engineering. Member AIAA.

¶Regents' Professor, School of Aerospace Engineering. Associate Fellow AIAA.

a flush-mounted side-wall microphone near the reattachment point location. It is seen in Fig. 2 that while there are some tunnel resonances present, they do not have a lot of acoustic power. Moreover, if the shear layer flapping phenomena of Ref. 5 were present, there would have been a peak near 250 Hz, which there is not.

The bottom wall, behind the step, is a porous metal plate through which secondary air or foreign gases may be blown. Provision has been made for blowing of air, CO₂, He, N₂, and H₂. The experimental part of the present paper is concerned only with the blowing of air.

The LV system is a two-component system (TSI 9100-7) fitted with a 4-watt argon ion laser (Spectra Physics 164-08); it operates in the backscatter mode, using two counter-type signal processors (TSI 1990A). Bragg cell frequency shifters (TSI 9108) in one beam of each of the two beam pairs permit a detection of reversed flow. The frequency shift can be adjusted to local flow conditions to permit acceptance of the entire velocity-related signal with maximum accuracy.

The LV system is mounted on an actuator, which is remotely controlled in three degrees of linear translation and manually controlled in tilt. The seed material used was TiO₂, with a particle size of 0.2 μ m. This gives a dynamic relaxation time of 0.46 μ s. This seed material was introduced at the tunnel inlet. The porous plate will plug if the injectant flow is seeded. As a consequence, there is no injectant seed and there will be a velocity bias near the wall in the injection cases. Unfortunately, no bias correction can be used since no information can be obtained about the unseeded injection flow.

The digital counter output delivers data when vertical and axial velocity signals are received within a coincidence window of 10 μ s. The data are digitally processed into probability density functions (pdf's) and joint pdf's, from which mean and rms velocities and shear stress are calculated. Typical axial velocity and joint vertical and axial velocity pdf's are shown in Figs. 3 and 4.

Analysis

Procedure

From prior experience with manipulation of near wakes by injection,⁶ the physical expectation is that the recirculation

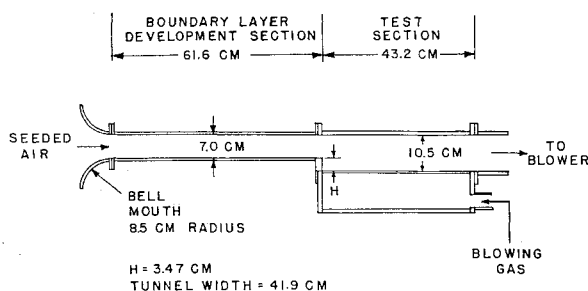


Fig. 1 Wind tunnel schematic.

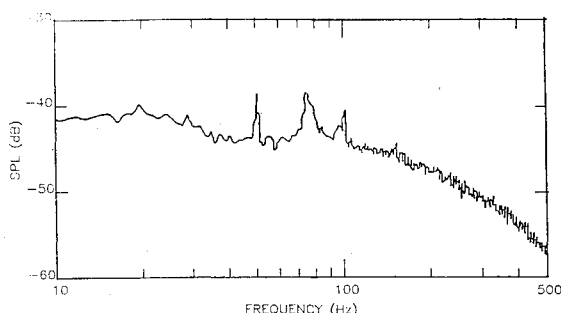


Fig. 2 Acoustic spectrum measured by flush-mount microphone on side wall near reattachment.

zone will be strongly modified by only moderate blowing. Typical SFRJ blowing velocities are less than 1 m/s, which is only of the order of 1% of the mean inlet flow speed. Nevertheless, some reasonably strong modifications to the flowfield are expected.

A two-equation turbulence model (k - ϵ) is used for the analysis of the current flowfield.^{7,8} With the exception of the new results introduced by wall blowing, this computation method has been used by many workers,^{3,4} and will not be fully documented here. A numerical code called TEACH,^{9,10} originally developed at Imperial College, is used for solution of the elliptic differential equations with appropriate boundary conditions; modifications introduced for calculation of the present problem resulted in a program to be designated TEACH-GT.

There are three primary modifications to the program. First, there is 7% turbulence kinetic energy (k) production added to the basic transport law to account approximately for pressure-velocity correlations.¹¹ This addition substantially improves the reattachment length prediction in the nonblown case.⁴ Secondly, for foreign-gas injection, a species conservation equation must be added and boundary conditions developed. Thirdly, with foreign-gas injection, the problem becomes one of variable density with its attendant difficulties.

Full documentation of the modifications is located in Ref. 12. Here only an outline will be given. The species concentration, C_i , for species i , is calculated from

$$\frac{\partial}{\partial x_j} (\bar{\rho} \bar{u}_j \bar{C}_i) = \frac{\partial}{\partial x_j} \left[\left(\frac{\mu + \mu_T}{\sigma_c} \right) \frac{\partial \bar{C}_i}{\partial x_j} \right] \quad (1)$$

$$\mu_T = 0.09 \bar{\rho} (k^2 / \epsilon)$$

An immediate problem will be seen in the use of Eq. (1) for variable density flows: it is inexact. The more popular approach¹³ is to presume that all dependent variables are interpreted as Favre-average (mass-weighted) quantities, with the exception of density, which is retained in its conventional time-average form. The problem then arises as to how to calculate mean density because, through the equation of state, the mean density depends upon both Favre-weighted concentrations and their fluctuations. One approach¹⁴ is to carry along another balance equation for the mean square concentration fluctuation which, together with an assumed shape for

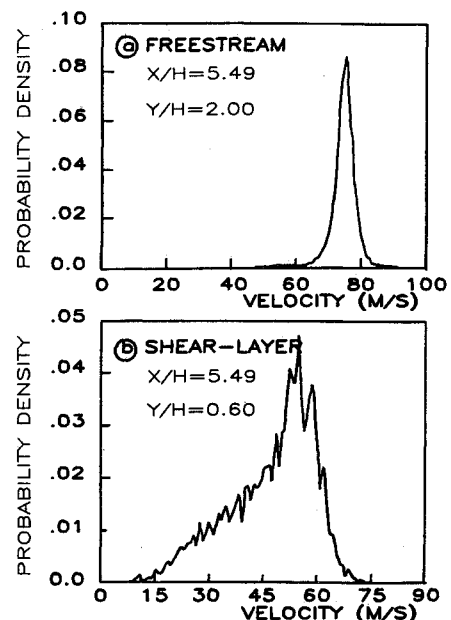


Fig. 3 Axial velocity pdf at two vertical locations at one axial station.

a probability distribution of the fluctuation, will allow a mean density calculation.

The equation for the concentration fluctuation variation was inserted into the program. The result was that the rms fluctuation level in density was too low ($<4\%$ of the mean density) to affect strongly the calculation of mean density. As a consequence, this calculation was dropped and it was considered that there is too little difference between conventional and Favre averages to warrant the sophistication at this time. When the reacting case is considered, this effect will, of course, have to be included.

Available measured profiles of the dependent variables are used to provide boundary conditions at the sudden expansion inlet. Outlet boundary conditions impose zero gradients at 24 step heights downstream of the step. Numerical calculations show this location to be sufficiently far downstream that the calculations in the recirculation region are not affected by the downstream conditions. For the solid surface boundary conditions, algebraic relations are used that are consistent with the "law of the wall." However, in the current case with wall blowing, some additional developments are necessary. Paralleling the Patankar and Spalding¹⁵ procedure and using data from Kays and Moffat¹⁶ to check the mass addition results, Ref. 12 contains a full description of the boundary conditions' development. At this point a difference occurs between true SFRJ simulation and the current simulator. Since the bottom wall of the apparatus is porous rather than solid, the air from the main channel can diffuse into the plate. In contrast, in an SFRJ the absolute air velocity perpendicular to the wall must be zero at the wall. The boundary condition used in this analysis is chosen to correspond to the actual experimental situation. The mass fraction of air is set zero at "minus infinity" rather than specifying zero transport rate at the wall.

A 31-axial by 41-vertical grid was used with an expanding grid in the axial direction. The expansion ratio was 1.15. This grid had achieved grid independence of the results in the no-bleed case.⁴ This grid dependence was not investigated separately for the bleed-flow cases. The effect of bleed flow is only felt close to the porous wall where it is incorporated in the boundary conditions. Since the bleed flow has a minimum effect on the gradients of the dependent variables as indicated by the results and since only the change in gradients will lead to a change in grid dependence, it is assumed that bleed has no effect on this dependence. The grid points next to the wall (one-half grid spacing away from the wall) were the points at which boundary conditions were applied. The balance equations used at these near-wall points were continuity, momentum, k , and C_i equations. The ϵ was calculated from the law of the wall relation

$$\epsilon = u_\tau^3 / \kappa y$$

where u_τ is the friction velocity calculated from

$$u_\tau = k^{1/2} C_\mu^{1/2}$$

with $C_\mu = 0.09$. A law of the wall including blowing was derived in Ref. 12, which yields the shear stress at the near-wall grid point. It is

$$\tau_w = \frac{\rho u C_\mu^{1/2} k^{1/2}}{(1/\kappa) \ln(Ey_+)} - \frac{\rho C_\mu^{1/2} k^{1/2}}{4} V_0 \frac{1}{\kappa} \ln(Ey_+) + \rho u V_0$$

Here E is the law of the wall constant, which is 9.5 for the no-blowing case but varies with injection rate. From Ref. 12, Fig. 5 shows this variation, which is able to match the results of Ref. 16. In the above $y_+ = y(C_\mu^{1/2} k)^{1/2} / \nu$. Correcting the shear stress at the near-wall point for the momentum due to injection, the wall shear stress is

$$\tau_0 = \tau_w - \rho_0 u V_0$$

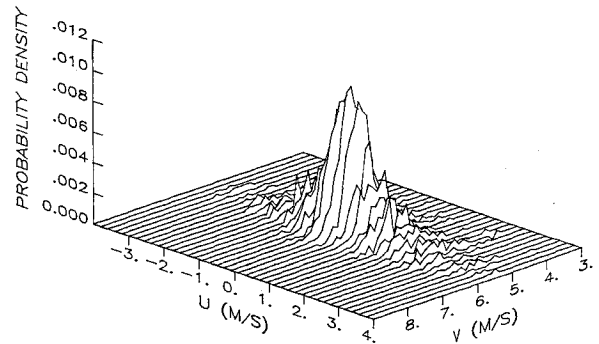


Fig. 4 Joint pdf of axial and vertical velocities.

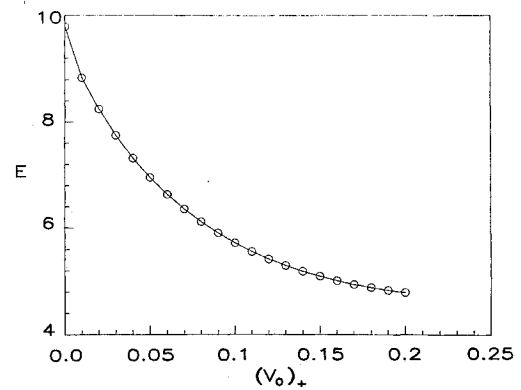


Fig. 5 Law of the wall constant as a function of blowing rate.

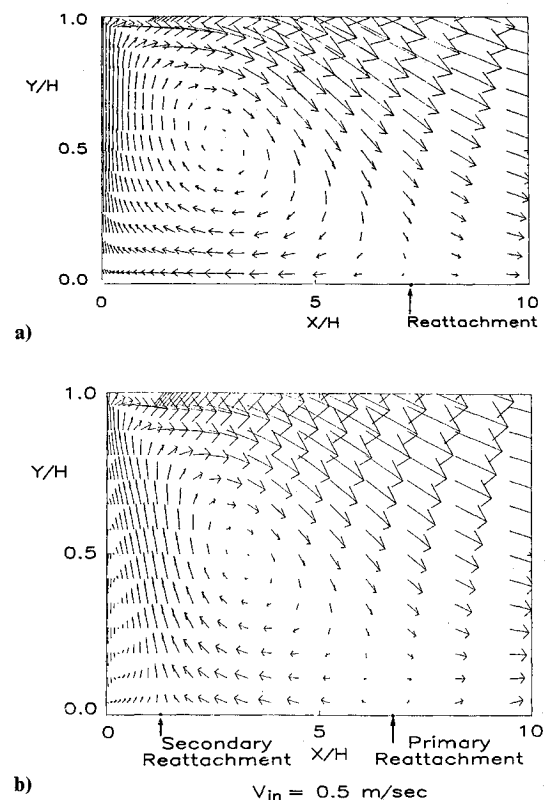


Fig. 6 Velocity vector plots comparing bleed against no bleed.

which is applied at the wall as a condition on the momentum equation.

The final piece of information needed is the wall condition of C_i . In Ref. 12 the condition needed is

$$C_{i0} = [(C_i - 1)/(1 + m_+ u_+)] \sigma_c + 1$$

where C_{i0} and C_i are the wall value and near-wall value of C_i , respectively. Here $m_+ = \rho_0 V_0 / u_+ \rho$ and $u_+ = u / u_+$. All non-subscripted quantities refer to the near-wall node points. This final equation is used together with the balance equation for C_i near the wall to determine both C_i and C_{i0} .

Results

Figure 6 shows a velocity vector plot of the recirculation zone comparing the no-bleed results with a bleed case, with CO_2 as the bleed gas. There are two dominant effects of bleed.

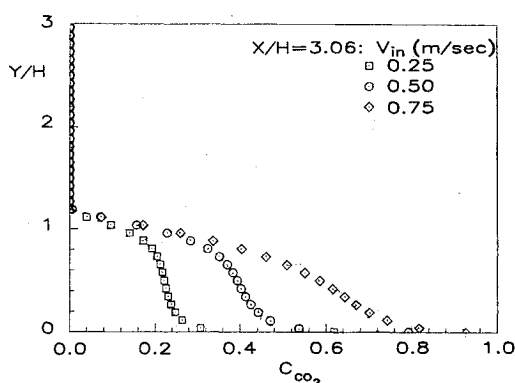


Fig. 7 Mass fraction of CO_2 against vertical distance for three bleed rates.

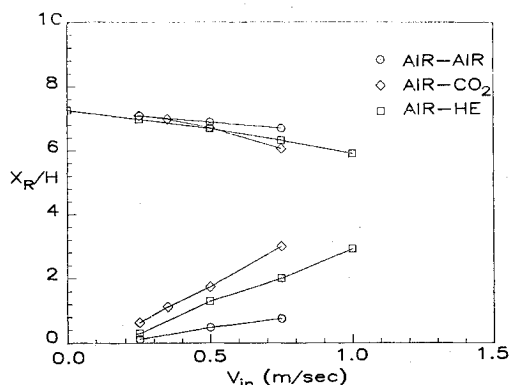


Fig. 8 Variations of flow reversal points with bleed rate and injectant type.

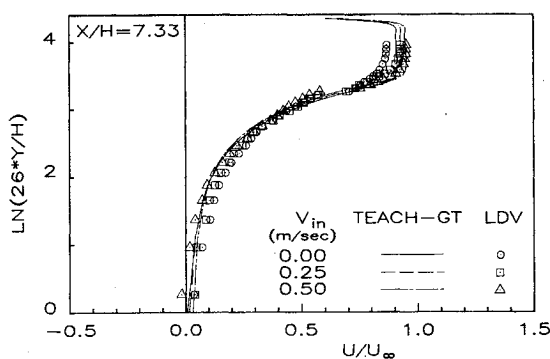


Fig. 9 Effect of bleed on mean axial velocity profiles.

First, there is the appearance of a second recirculation zone. Second, the extent of the primary recirculation zone is lessened, with much less backflow. With bleed there is more "up and away" flow than a dominant recirculation flow. Thus, even at low blowing velocities, the recirculation zone is being "blown off." This is also illustrated in Fig. 7, where CO_2 mass fractions are displayed at about the mid-length point of the original recirculation zone. The flat profiles at low injection rate are indicative of a well-stirred recirculation zone, whereas the smooth diffusion profiles at high injection rate indicate near blowoff of the recirculation flow.

This phenomenon may have important implications for the flame stabilization characteristics for these flows. Presumably, anchoring a flame in this region requires two things—low velocity and a favorable (nearly stoichiometric) fuel (injectant)/air ratio. Near blowoff, a favorable mixture may occur somewhere in the flowfield, but the velocity may be too high in the downstream direction.

Shown in Fig. 8 are the variations in the position of the two flow reversal (loosely called reattachment) points with injection rate for three different injection rates. The influence of injection is more nearly a volume flow than a mass flow phenomenon for a given injectant velocity, as expected. Notice that the downstream flow reversal point movement is much weaker than the near-step point movement.

Other changes in the flowfield with injection are much less pronounced. For example the mean streamwise velocity is little affected, as seen in Fig. 9. The maximum value of the shear stress at any axial location is shown in Fig. 10 for the case of air injection. Again, there is little effect of injection on the primary shear layer.

The main conclusion of the analysis is that for the blowing velocities of interest there is little structural change of the main mixing layer but that there can be a large change in the recirculatory region structure. This change may be deleterious to the flame-holding capacity of the region due to a reduced residence time of fuel in this region, but firm conclusions will have to await further analysis and experimentation.

Experimental Results

Prior results⁴ obtained in the no-bleed case using hot-wires and pitot probes were checked with the LV system. A typical comparison of axial velocity obtained with these methods is shown in Fig. 11, along with the analytical curve. Several stations were compared to lend confidence in the LV results. The development of the axial velocity profile with downstream distance is shown in Fig. 12, all data being obtained with the LV for the no-bleed case. Reattachment of the shear layer occurs at 7.3 step heights downstream of the step, and there is a single observable time mean recirculation zone, in accordance with calculation.

Two bleed cases, both with air as the injectant, are reported here. The injectant velocities were nominally 0.25 and 0.50

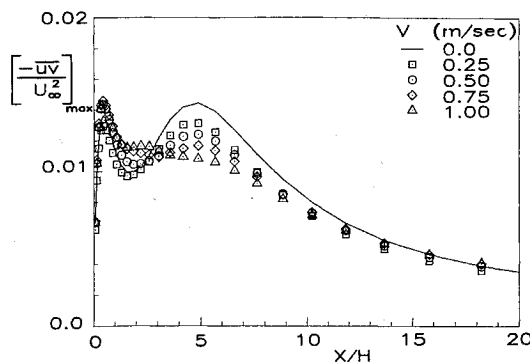


Fig. 10 Maximum shear stress against axial position as a function of bleed rate.

m/s. There is a mild axial variation in the bleed velocity due to a small pressure gradient in the tunnel. However, the pressure drop across the porous plate is large compared with the pressure variation in the tunnel.

First, notice the location of the zero axial velocity line in Fig. 13. In accord with analytical expectations, there is very little effect of blowing on this line's position. Referring back to the calculations of Fig. 6 and tracing the zero axial velocity line on the upper edge of the recirculation zones, there was little effect to be expected by blowing. Prediction of the analysis that there would be a mild shift of the downstream flow reversal point toward the step did not materialize. Figure 13 shows that this point is independent of the blowing rate.

As predicted, a second recirculation zone appears experimentally upon injection. This is shown in Fig. 14, viewing the x/H position of 1.06. It should be borne in mind that the $k-\epsilon$ modeling used is least accurate near positions of flow reversal because of the use of law of the wall boundary conditions. The fact that two recirculation regions are found experimentally lends some more confidence in the calculation method, even though the calculation only predicts a secondary recirculation zone length of $x/H = 0.4$. Importantly, the non-shift of the zero axial velocity line and the diminution in size of the primary recirculation zone confirms the analytical prediction that blowing probably reduces the flame-holding effectiveness of the region.

The calculation method does come under some "stress," however, when one looks at the predictions of shear stress. Shown in Fig. 15 is the maximum value of the shear stress at

each axial location. Recall that the analysis predicts very little change with blowing, with a mild reduction in the absolute value of the maximum with an increase in blowing rate. In Fig. 15, there is a mild increase in the value of shear stress at both low and high x/H but little change in the absolute maximum value. This indicates an increase in turbulent transport rates with a blowing increase. Such behavior would be beneficial to flame stabilization, in contrast to the opposing effect of diminution of the recirculatory region extent. Firm conclusions, however, must await further Rayleigh scattering measurements of species transport.

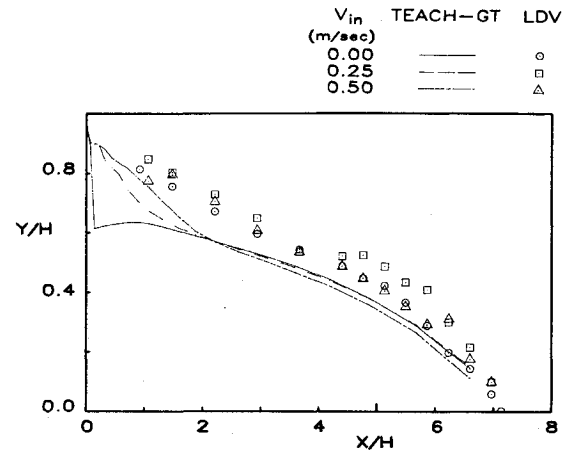


Fig. 13 Location of the zero axial velocity line vs bleed rate.

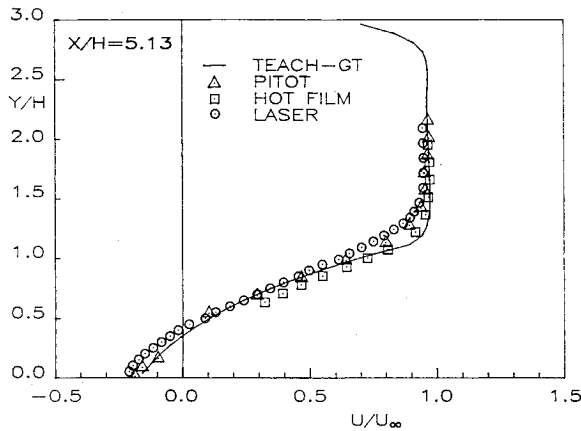


Fig. 11 Comparison of various measurements and theory for the axial mean velocity profile.

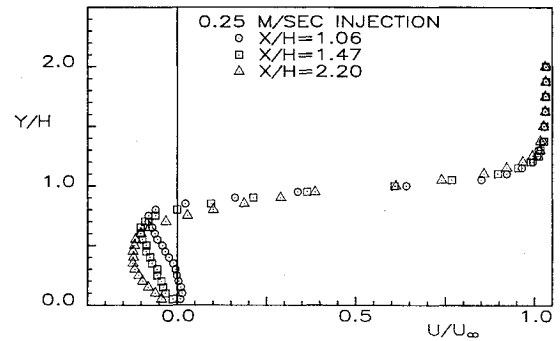


Fig. 14 Mean axial velocity vs vertical distance with bleed flow.

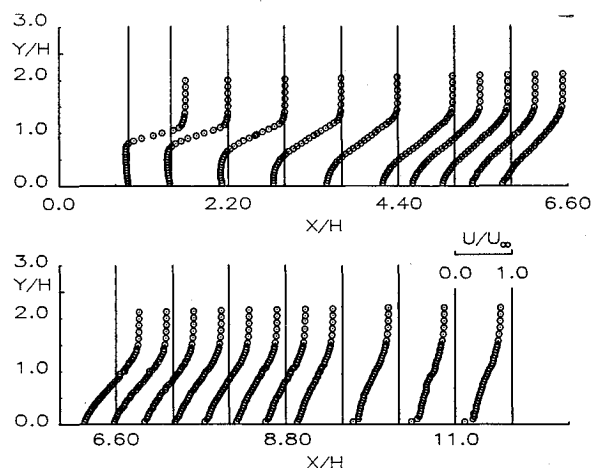


Fig. 12 Development of the mean axial velocity profile with no bleed against axial distance.

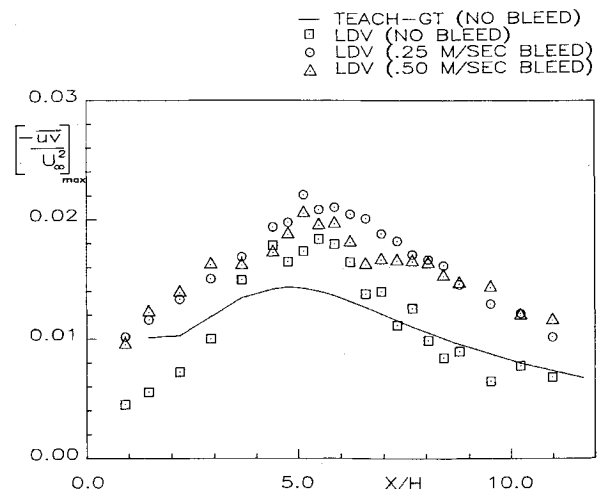


Fig. 15 Experimental variation of the maximum shear stress with bleed.

Conclusions

Blowing at the wall behind a backward-facing step in a simulation of the SFRJ flame stabilization region produces the following effects:

- 1) A second recirculation zone appears.
- 2) There is diminution of extent of the primary recirculation zone with increased blowing and a lessening of the recirculatory strength, which is viewed as destabilizing from a flame-holding point of view.
- 3) Turbulent transport rates appear to increase with a blowing rate increase that is viewed as stabilizing insofar as flame holding is concerned.

Future experiments must concentrate on species concentration measurements made simultaneously with velocity measurements to confirm or deny the mass transport conclusion intimated previously.

Acknowledgments

This work is supported by the Air Force Office of Scientific Research under Grant No. 83-0356. Dr. Leonard H. Caveny is the program monitor.

References

- ¹Netzer, D.W., "Modeling Solid-Fuel Ramjet Combustion," *Journal of Spacecraft and Rockets*, Vol. 14, Dec. 1977, pp. 762-766.
- ²Eaton, J.K. and Johnston, J.P., "A Review of Research on Subsonic Turbulent Flow Reattachment," *AIAA Journal*, Vol. 19, Sept. 1981, pp. 1093-1100.
- ³Kline, S.J., Cantwell, B.J., and Lilley, G.M., "1980-81 AFOSR HTTM-Stanford Conference on Complex Turbulent Flows," Vol. I, Stanford University, Stanford, CA, 1981, p. 287.
- ⁴Walterick, R.E., Jagoda, J.I., Richardson, C.R.J., de Groot, W.A., Strahle, W.C., and Hubbart, J.E., "Experiments and Analysis on Two-Dimensional Turbulent Flow over a Backward Facing Step," AIAA Paper 84-0013, 1984.
- ⁵Driver, D.M., Seegmiller, H.L., and Marvin J., "Unsteady Behavior of a Reattaching Shear Layer," AIAA Paper 83-1712, 1983.
- ⁶Walterick, R.E., Hubbart, J.E., and Strahle, W.C., "Base Burning Performance at Mach 3," *AIAA Journal*, Vol. 20, July 1982, pp. 986-991.
- ⁷Jones, W.P. and Launder, B.E., "The Prediction of Laminarization with a Two Equation Model of Turbulence," *International Journal of Heat and Mass Transfer*, Vol. 15, 1972, pp. 301-314.
- ⁸Jones, W.P. and Launder, B.E., "The Calculation of Low Reynolds Number Phenomena with a Two-Equation Model of Turbulence," *International Journal of Heat and Mass Transfer*, Vol. 16, 1973, pp. 1119-1130.
- ⁹Gosman, A.D. and Pun, W.M., "Calculation of Recirculating Flows," Mechanical Engineering Department Report, Imperial College, London, 1973.
- ¹⁰*Measurements and Predictions of Complex Turbulent Flows*, Vols. 1 and 2, von Kármán Institute for Fluid Dynamics, Lecture Series 1980-83, Feb. 11-15, 1980.
- ¹¹Strahle, W.C., "Velocity-Pressure Gradient Correlation in Reactive Turbulent Flows," *Combustion Science and Technology*, Vol. 32, 1983, pp. 289-305.
- ¹²Richardson, J.C.R., "Analysis of a Sudden Expansion Flow in a Two Dimensional Duct With and Without Side-Wall Injection Using the $k-\epsilon$ Turbulence Model," Ph.D. Dissertation, Georgia Institute of Technology, Atlanta, GA, 1984.
- ¹³Kent, J.H. and Bilger, R.W., "The Prediction of Turbulent Diffusion Flame Fields and Nitric Oxide Formation," *16th Symposium (International) on Combustion*, The Combustion Institute, Pittsburgh, PA, 1977, pp. 1643-1656.
- ¹⁴Bilger, R.W., "Turbulent Flows with Nonpremixed Reactants," in *Turbulent Reacting Flows*, edited by Williams and Libby, Springer-Verlag, Berlin, 1980, pp. 65-114.
- ¹⁵Patankar, S.V. and Spalding, D.B., *Heat and Mass Transfer in Boundary Layers*, 2nd ed., Intertext Books, London, 1970.
- ¹⁶Kays, W.M. and Moffat, R.J., "The Behavior of Transpired Turbulent Boundary Layers," *Studies in Convection*, Vol. 1, edited by B.E. Launder, Academic Press, New York, 1975.

From the AIAA Progress in Astronautics and Aeronautics Series . . .

TRANSONIC AERODYNAMICS—v. 81

Edited by David Nixon, Nielsen Engineering & Research, Inc.

Forty years ago in the early 1940s the advent of high-performance military aircraft that could reach transonic speeds in a dive led to a concentration of research effort, experimental and theoretical, in transonic flow. For a variety of reasons, fundamental progress was slow until the availability of large computers in the late 1960s initiated the present resurgence of interest in the topic. Since that time, prediction methods have developed rapidly and, together with the impetus given by the fuel shortage and the high cost of fuel to the evolution of energy-efficient aircraft, have led to major advances in the understanding of the physical nature of transonic flow. In spite of this growth in knowledge, no book has appeared that treats the advances of the past decade, even in the limited field of steady-state flows. A major feature of the present book is the balance in presentation between theory and numerical analyses on the one hand and the case studies of application to practical aerodynamic design problems in the aviation industry on the other.

Published in 1982, 669 pp., 6×9, illus., \$45.00 Mem., \$75.00 List

TO ORDER WRITE: Publications Dept., AIAA, 1633 Broadway, New York, N.Y. 10019